



This is a repository copy of *A method to determine acoustic properties of solids and its application to measuring oil film thickness in bearing shells of unknown composition.*

White Rose Research Online URL for this paper:

<https://eprints.whiterose.ac.uk/185783/>

Version: Accepted Version

---

**Article:**

Beamish, S., Reddyhoff, T., Hunter, A. et al. (1 more author) (2022) A method to determine acoustic properties of solids and its application to measuring oil film thickness in bearing shells of unknown composition. *Measurement*, 195. 111176. ISSN 0263-2241

<https://doi.org/10.1016/j.measurement.2022.111176>

---

Article available under the terms of the CC-BY-NC-ND licence  
(<https://creativecommons.org/licenses/by-nc-nd/4.0/>).

**Reuse**

This article is distributed under the terms of the Creative Commons Attribution-NonCommercial-NoDerivs (CC BY-NC-ND) licence. This licence only allows you to download this work and share it with others as long as you credit the authors, but you can't change the article in any way or use it commercially. More information and the full terms of the licence here: <https://creativecommons.org/licenses/>

**Takedown**

If you consider content in White Rose Research Online to be in breach of UK law, please notify us by emailing [eprints@whiterose.ac.uk](mailto:eprints@whiterose.ac.uk) including the URL of the record and the reason for the withdrawal request.



[eprints@whiterose.ac.uk](mailto:eprints@whiterose.ac.uk)  
<https://eprints.whiterose.ac.uk/>

---

# A method to determine acoustic properties of solids and its application to measuring oil film thickness in bearing shells of unknown composition

Beamish S<sup>1</sup>, Reddyhoff T<sup>2</sup>, Hunter A<sup>1,3</sup> and Dwyer-Joyce RS<sup>1</sup>  
Measurement, 2022

<sup>1</sup> The Leonard Centre for Tribology, Department of Mechanical Engineering, University of Sheffield, UK

<sup>2</sup> Department of Mechanical Engineering, Imperial College, London, UK

<sup>3</sup> Peak to Peak Measurement Solutions Ltd, Sheffield, UK.

## Abstract

Acoustic impedance is an important property used to interpret acoustic reflection measurements in tests to determine oil film thickness, a critical parameter dictating efficiency and wear rates of lubricated components. A new method to measure acoustic impedance of solid media, based on the well-established spring model, is described. The advantage of this method over existing techniques is that it can be applied to thin, multi-layered materials where individual reflections cannot be distinguished, common in many tribological systems such as bearings, piston rings and piston liners. The method is demonstrated experimentally for a range of materials. Results compare well with values calculated independently from acoustic velocity and density. The method has been applied to a bearing test rig to determine acoustic impedance of a thin-walled bearing. This study demonstrates that the technique is capable of measurements in dynamic systems and where traditional methods of calculating acoustic impedance are not feasible.

---

## 1. Introduction

### *Acoustic Impedance*

Acoustic impedance is a measure of a material's resistance to acoustic flow and is most simply defined as the product of density and acoustic velocity in that material [1]:

$$z = \rho c \quad (1)$$

Where  $z$  is acoustic impedance,  $\rho$  is density and  $c$  is acoustic velocity.

Modelling acoustic wave behaviour often requires the acoustic impedance of the materials to be known, primarily as it affects how the sound is transmitted between materials. In many applications the parameter can be found by equation 1, with acoustic velocity obtained by a time-of-flight measurement and density by measuring the material's weight and volume (by geometry or measuring displacement) or obtained from literature if it is a more common material.

Additional techniques for measuring acoustic impedance have been developed recently. For example, Hoche et al. [2] applied a multiple reflection method using a 2 MHz centre frequency transducer and achieved measurement accuracies to within 0.12% of the true value. However, this method is only suitable measuring the acoustic impedance for liquids. Bianco et al. measured the acoustic impedance of pavements using pressure-velocity probes via a modified version of the Adrienne method. This compared the power spectra from the incident and reflected acoustic waves. Acoustic impedance can then be calculated by the ratio between local pressure and particle velocity. This technique requires a large microphone suspended in air at a known distance above the material, which in their study this distance was 160mm [3].

An accurate value of acoustic impedance is particularly important in ultrasonic thin film thickness measurements and is required for the popular spring amplitude and phase models. In 2020, Yu et al. presented another method to directly calculate thickness in thin films without requiring acoustic impedance, known as the exact-complex technique. However, the authors note that measurement uncertainty may be increased as it is a combination of the uncertainties in both the amplitude and phase shift measurements [4].

Unfortunately, applying previous methods to determine acoustic impedance is not always feasible. For example, many tribological components such as bearings, piston rings and piston liners are coated with a thin layer of material, such as diamond-like carbon (DLC), chromium ceramic or complex multi-phase alloys such as leaded bronze [5, 6, 7]. With thin layers, individual acoustic reflections are no longer distinct, making a direct measurement of acoustic velocity via a time-of-flight technique impossible [8]. Furthermore, depending on the deposition technique, the layer acoustic impedance may be different to the acoustic impedance of the bulk material. Thus, an alternative technique would be required.

The acoustic impedance of individual materials in a perfectly coupled multi-layer system can also be calculated by observing the proportion of the acoustic wave reflected at the boundary, known as the reflection coefficient,  $R$  [9, 10]:

$$R = \frac{z_2 - z_1}{z_2 + z_1} \quad (2)$$

Where  $z_1$  and  $z_2$  are the acoustic impedances of each medium. Provided the acoustic impedance of one material is known, this equation allows the acoustic impedance of the other material to be calculated.

Studying equation 2, one may see that a large acoustic impedance mismatch between materials will cause almost all the acoustic energy to be reflected at the interface if  $z_2 \gg z_1$  or  $z_1 \gg z_2$ .

---

Thus, accurate measurements rely on the acoustic impedance of the materials to be similar in magnitude. By extension, this means higher impedance materials such as metals require the other material to be solid, and only low impedance solids such as rubbers and polymers can be measured when the first medium is a liquid.

However, real solid surfaces are not perfectly flat and in most cases this roughness cannot be ignored. When two materials are pressed together it is therefore not possible to achieve a perfect interface. Air gaps between the peaks of contacts will always be present. As such, solid-solid interfaces require an intermediate coupling layer to create a perfect interface between the two media, as shown in figure 1. This requirement is somewhat convenient, as the interface in many tribological applications such as bearings, is a metal-on-metal contact separated by a thin layer of lubricant.

As the stiffness of the liquid layer is far lower than that of the solid materials, it therefore dominates the signal response at the interface and cannot be ignored. Pedrix et al [11] modelled this behaviour and measured the change in reflection due to the intermediate layer. However, their technique, which observed the decrease in response as the fluid thickness matched the resonant frequency of the acoustic wave, required the thickness of the coupling layer to be known, consistent and uniform across the measurement area. This is often a challenging requirement outside of lab conditions and in real engineering components.

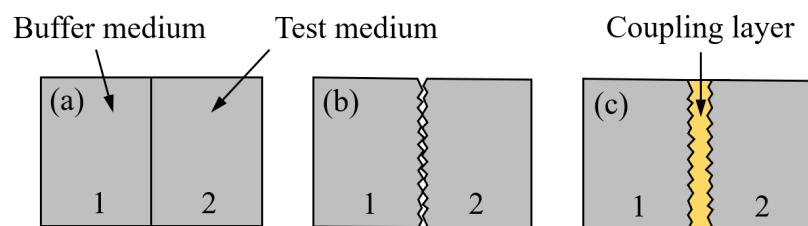


Figure 1. Schematic diagram of (a) theoretical perfectly coupled interface, (b) real solid interfaces where contact surfaces are rough, (c) real solid interfaces including a coupling layer.

### *The Spring Model*

When the thickness of a layer between two solid bodies is thin (compared to the wavelength of the acoustic signal) the stiffness of this layer dominates signal response, affecting both the proportion of the signal that is reflected at this layer and the signal's phase. Conversely, the effect of mass and damping may be assumed to be negligible at this scale. As such the acoustic response may be accurately modelled using a quasi-static spring model.

This technique has been used successfully to investigate a wide range of tribological problems, including the study of adhesive bonds [12, 13, 14], cracks under compressive loading [15, 16], contact phenomena in rough surfaces [17, 18, 19, 20, 21] and lubricant film thickness [22, 23, 24]

The above studies which model the response of the layer require that the impedance of the materials each side of the interface are known. In the present study, the spring model has been applied to relate the amplitude and phase shift of the reflected ultrasonic wave to the acoustic properties of the materials either side of the layer. This is first demonstrated by observing the signal response of a thin lubricant layer between two plates under static conditions. The approach has then been used in the practical example of an engine bearing shell where the acoustic impedance of the multi-layer shell is unknown.

## 2. Ultrasonic Reflection at a Thin Film

When an ultrasonic pulse is incident on a thin layer, part is transmitted through, part is reflected back. Measured against the incident wave, the reflected wave has reduced amplitude and an associated phase shift. This is shown in figure 2, where the effect of layer thickness is also shown.

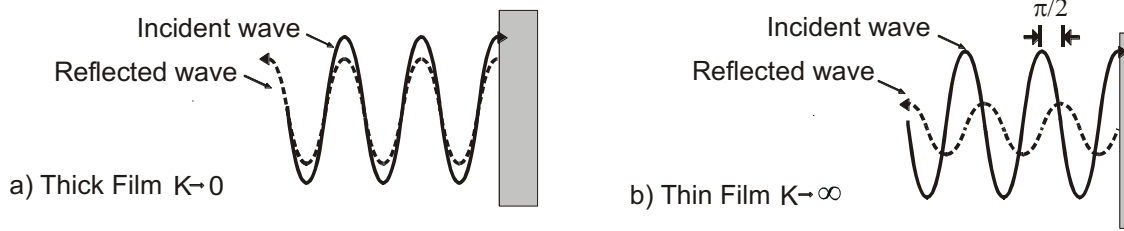


Figure 2. A diagram of both the incident and reflected waves at a thick (a) and thin (b) intermediate layer, with the corresponding change in phase and amplitude shown, where  $K$  is layer stiffness. [8]

By considering the balance of forces and compatibility at the layer boundaries during the passage of the wave, the reflection coefficient at an interface may be calculated by the following [12, 13]:

$$R = \frac{(z_1 - z_2) + iz_1 z_2 \left(\frac{\omega}{K}\right)}{(z_1 + z_2) + iz_1 z_2 \left(\frac{\omega}{K}\right)} \quad (3)$$

For which  $K$  is layer stiffness and  $\omega$  is the angular frequency of the ultrasonic wave.  $R$  is a complex quantity containing amplitude and phase information. Reflection coefficient amplitude  $|R|$  represents the reduction in amplitude in the reflected wave while the phase shift  $\Phi_R$  represents the phase difference between the incident and reflected waves. This relation holds for both longitudinal and shear waves, although for shear waves  $K$  represents interfacial shear stiffness, as opposed to longitudinal stiffness [25]. It will be shown later that the stiffness terms can be eliminated; thus, the same approach can be applied to both shear and longitudinal waves, however this work will focus on longitudinal waves.

As layer thickness increases, the stiffness of this layer decreases. The phase difference, between an incident and reflected wave, thus varies from 0 for a thick film ( $K \rightarrow 0$ ), to  $\pi/2$  for a thin film ( $K \rightarrow \infty$ ). This is shown graphically in figure 2.

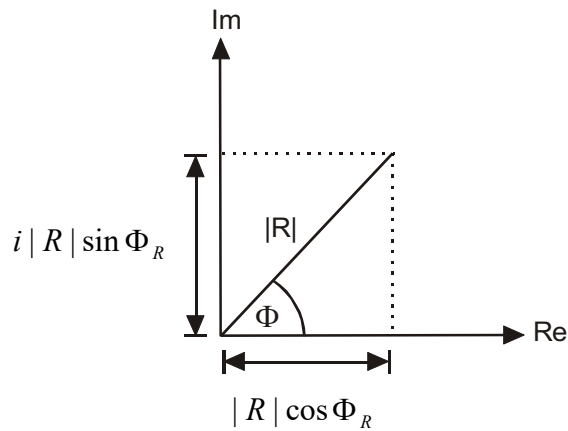


Figure 3. Complex representation of reflection coefficient

As shown in figure 3,  $R$  has the form:

$$R = |R| \cos \Phi_R + i|R| \sin \Phi_R \quad (4)$$

Combining Equations (3) and (4):

$$\begin{aligned} & \left[ (z_1 + z_2)|R| \cos \Phi_R - z_1 z_2 \left( \frac{\omega}{K} \right) |R| \sin \Phi_R - (z_1 - z_2) \right] \\ & + i \left[ z_1 z_2 \left( \frac{\omega}{K} \right) |R| \cos \Phi_R + (z_1 + z_2)|R| \sin \Phi_R - z_1 z_2 \left( \frac{\omega}{K} \right) \right] = 0 \end{aligned} \quad (5)$$

Since both real and imaginary parts must be equal to zero, equation (5) can be rewritten as a pair of simultaneous equations:

$$(z_1 + z_2)|R| \cos \Phi_R - z_1 z_2 \left( \frac{\omega}{K} \right) |R| \sin \Phi_R - (z_1 - z_2) = 0 \quad (6)$$

$$z_1 z_2 \left( \frac{\omega}{K} \right) |R| \cos \Phi_R + (z_1 + z_2)|R| \sin \Phi_R - z_1 z_2 \left( \frac{\omega}{K} \right) = 0 \quad (7)$$

The frequency stiffness term can be eliminated from equations (6) and (7) to give an equation relating reflection coefficient amplitude and phase to the material properties:

$$(z_1 + z_2)|R| \cos \Phi_R - \frac{(z_1 + z_2)|R|^2 \sin^2 \Phi_R}{(1 - |R| \cos \Phi_R)} - (z_1 - z_2) = 0 \quad (8)$$

Equation (8) can be simplified to give a quadratic equation in  $|R|$ :

$$(z_1 + z_2)|R|^2 - 2z_1|R| \cos \Phi_R + (z_1 - z_2) = 0 \quad (9)$$

The quadratic formula can be applied to equation (9) to obtain an expression for reflection coefficient amplitude:

$$|R| = \left( \frac{1}{1 + \frac{z_2}{z_1}} \right) \cos \Phi_R \pm \sqrt{\left( \frac{1}{1 + \frac{z_2}{z_1}} \right)^2 \cos^2 \Phi_R - \left( \frac{1 - \frac{z_2}{z_1}}{1 + \frac{z_2}{z_1}} \right)} \quad (10)$$

It is important to note from equation (10) that the relationship between amplitude and phase is independent of layer properties, layer thickness or ultrasonic frequency and only depends on acoustic impedances of the materials either side of the layer.

If the materials either side of the layer are identical ( $z_1 = z_2$ ), equation (10) reduces to:

$$|R| = \cos \Phi_R \quad (11)$$

Equation (10) can be rearranged to provide an expression for the acoustic impedance of the second material  $z_2$ :

$$z_2 = z_1 \frac{|R|^2 - 2|R| \cos \Phi_R + 1}{1 - |R|^2} \quad (12)$$

This relationship is the foundation of the acoustic impedance measurement technique outlined in this paper. With this, a simultaneous reflection coefficient amplitude and phase measurement allows an acoustic impedance measurement of the second material independent of the coupling material, provided the acoustic impedance of the first material is known.

### 3. Measurement of Reflection Coefficient Amplitude and Phase

To determine reflection coefficient amplitude, the signal response may be compared against a reference measurement in which a known proportion of the signal is reflected at the interface:

$$R(f) = \frac{A(f)}{A_0(f)} R_0(f) \quad (13)$$

For which  $A(f)$  is the response amplitude reflected at the coupling layer,  $A_0(f)$  is the reference signal amplitude and  $R_0$  is the reference signal reflection coefficient.

Similarly, reflection coefficient phase can be determined by comparing the phase difference between the signal response at the coupling layer and a reference signal:

$$\Phi_R(f) = \varphi(f) - \varphi_0(f) \quad (14)$$

For which,  $\phi(f)$  is the signal phase reflected at the interface of interest and  $\phi_0(f)$  is reference signal phase.

#### 4. Measurement Apparatus

In the present study a commercial longitudinal transducer with a centre frequency of 1.25 MHz was used. Configured in pulse-echo mode, the transducer could both generate and receive the ultrasonic signal via an ultrasonic pulser receiver (UPR). The transducer produced pulses which contained energy distributed over a broad frequency bandwidth around the centre frequency.

This transducer was bonded to a steel delay line (operating as the buffer) which has an acoustic impedance of 46 MRayls. This delay line interfaces with a test medium via an intermediate oil coupling layer. The test medium can be easily swapped so that a range of materials could be investigated. A diagram of the measurement apparatus is shown in figure 4.

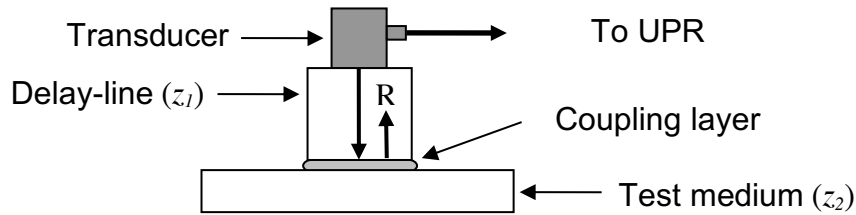


Figure 4. Diagram of impedance measuring set up.

#### 5. Test Method

An oil layer was deposited on to a range of test media (aluminium, brass, glass, Perspex and steel). The transducer and delay-line assembly was then positioned onto the test medium, and reflected pulses were captured and stored. An air reference signal was also obtained, for which the test medium was removed, and the delay line cleaned to remove any remaining oil. The acoustic impedance of air is orders of magnitude smaller than the steel delay line, thus it may be assumed that this solid-air interface is perfectly reflective [20].

A Fast Fourier Transform (FFT) was performed to convert each recording into the frequency domain, which contains both amplitude and phase information. The reflection coefficient was determined by dividing the amplitude spectrum of the oil film measurement by the air reference signal, as described in equation (13). Similarly, the phase difference was found by subtracting the oil film phase difference spectrum by the phase difference spectrum of the air reference signal, as in equation (14). These values were then applied to equation (12) to calculate the acoustic impedance of the test medium.

---

To compare results against conventional techniques, the density and acoustic velocity of each material was also measured. Density was calculated by measuring mass and volume, whereas acoustic velocity was taken via a time-of-flight method. The test media were simple rectangular plates, as such volume could be taken via their geometry.

## 6. Results

### 6.1. Reflection Amplitude and Phase

The reflected time domain signal response of each test case is presented in figure 5, along with the air reference signal. As predicted, a clear decrease in amplitude is observed for each material when compared against the reference amplitude. Similarly, the signal responses have shifted along the time domain compared to the air reference, indicating a phase change. The magnitude of both amplitude reduction and phase change is due to both the acoustic mismatch and the thickness of the oil layer and therefore they must be decoupled to determine acoustic impedance.

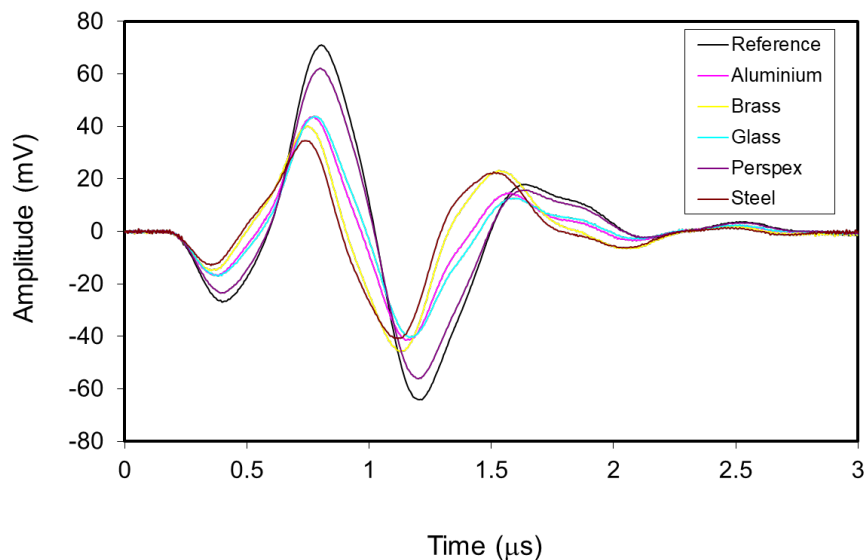


Figure 5. Reflected pulses from coupling layer, between steel delay line and material specimens.

The frequency amplitude and unwrapped phase spectra shown in figure 6a and figure 6b respectively were obtained by applying an FFT to the time-domain signals in figure 5. The phase results in figure 6b follow a saw-tooth profile as the phase change is wrapped between  $-\pi$  and  $\pi$  radians.

Reflection coefficient was calculated for each test case by dividing the amplitude by the reference at each point across the frequency range. The resultant curves in figure 6c show a smooth frequency dependence around the transducer centre frequency (approximately 0.5 MHz to 2 MHz). Results outside of this range may be ignored due to the low signal-noise ratio.

Similarly, phase shift is obtained by subtracting the reference phase from the phase measurement for each test case. Figure 6d shows that, as with reflection coefficient amplitude, phase change exhibits a smooth frequency dependence around the transducer centre frequency.

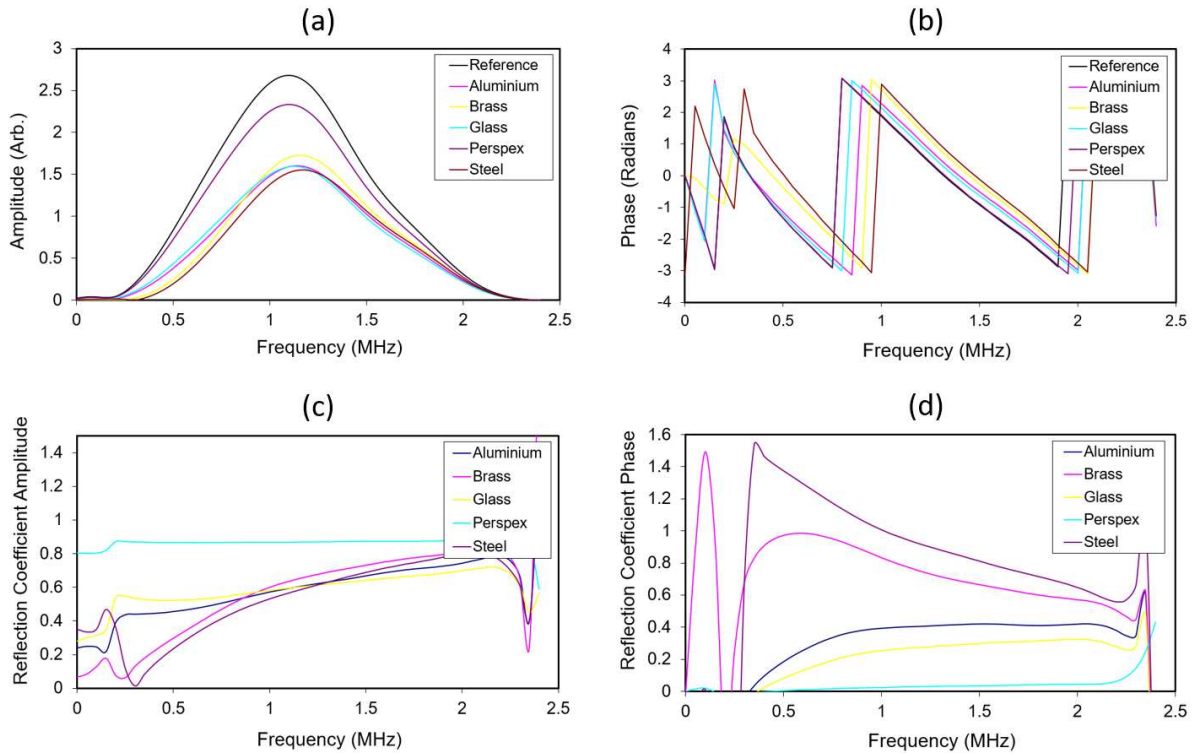


Figure 6. (a) Amplitude, (b) phase, (c) reflection coefficient amplitude and (d) reflection coefficient phase spectra for reflected pulses from oil layer, between steel delay line and material specimens.

### 6.2. Acoustic Impedance

As the reflection coefficient amplitude and phase measurements had been obtained, acoustic impedance could be determined via equation 12 for each material at all measured frequencies. Figure 7 shows the acoustic impedance calculated across the full measured frequency range.

Acoustic impedance is consistent across the usable transducer frequency range, indicated by a flat line over this region. This indicates that the presented technique enables acoustic impedance measurements independent of transducer frequency. Also notable is that the measurement for low acoustic impedance materials such as Perspex appear to be more consistent across the frequency spectrum in absolute terms compared to higher acoustic impedance materials such as steels. However, variations appear more consistent between materials when comparing uncertainties as a percentage.

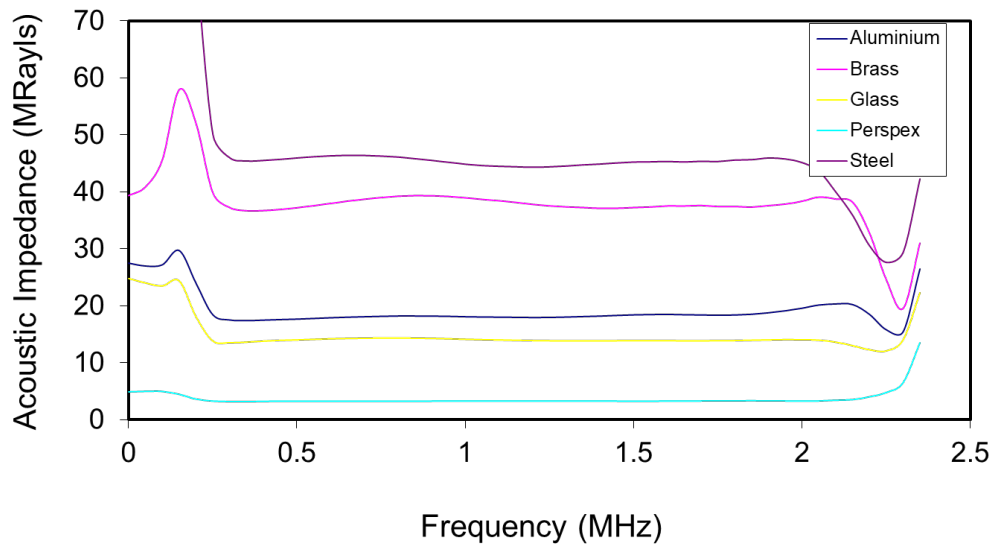


Figure 7. Acoustic impedance values deduced from reflection coefficient amplitude and phase.

To obtain a single value for each material, the acoustic impedance was averaged between 0.5 MHz and 2 MHz. Results are displayed in table 1, along with measurements obtained from the acoustic velocity-density method (as described in equation 1) and values obtained from literature. Differences between methods are small and it is likely that variation is due to errors in each technique, such as non-uniform material geometries when calculating volume or differences in exact material specifications compared to those used in values provided by datasheets. It is estimated that uncertainty in the spring model method amounts to less than 5%.

Table 1. Values of acoustic impedance for the test specimens measured via the presented spring model method, calculated via the acoustic velocity-density method, and taken from literature [1].

Material	Acoustic Impedance (MRayls)		
	Measured	Calculated	Data book
Aluminium	18.61	17.33	17.06
Brass	36.56	35.89	37.30
Glass	14.08	13.50	18.00
Perspex	3.78	3.17	3.22
Steel	42.96	46.17	45.63

### 6.3. Density

In this investigation there was a clear separation between the first and second reflected waves. As such, the acoustic velocity may be simply obtained by dividing the path length of the acoustic wave by the time taken between reflections. Then, via equation 1, density may be obtained using this acoustic velocity value and the acoustic impedance calculated using the spring model method. The resultant density values for each material are shown in table 2, along with density values calculated via the weight and geometry method and obtained from literature. As with acoustic impedance measurements, good agreement between methods is evident.

Table 2. Density values for the measured specimens.

Material	Density ( $\text{kgm}^{-3} \times 10^{-3}$ )		
	Measured	From Weight & Geometry	Data book
Aluminium	28.81	26.83	27.85
Brass	86.05	84.47	84.20
Glass	26.10	25.02	34.22
Perspex	11.96	11.71	11.79
Steel	72.55	77.96	77.6

#### 6.4. Argand Plot of Data

As reflection coefficient contains both amplitude and phase information, it may be conveniently represented as a vector on a complex plane using the same data. The length of this vector is equal to reflection coefficient amplitude and the angle represents its phase. The relationship between phase and amplitude (equation 10), which depends only on acoustic properties of the two solids can thus be plotted as a locus on the complex plane. The locus for each material specimen is shown in figure 8. This locus forms a semi-circular arc, initiating at the point of minimum reflection coefficient amplitude, progressing as frequency-thickness increases to infinity, at which point reflection coefficient amplitude reaches unity and phase is equal to 0.

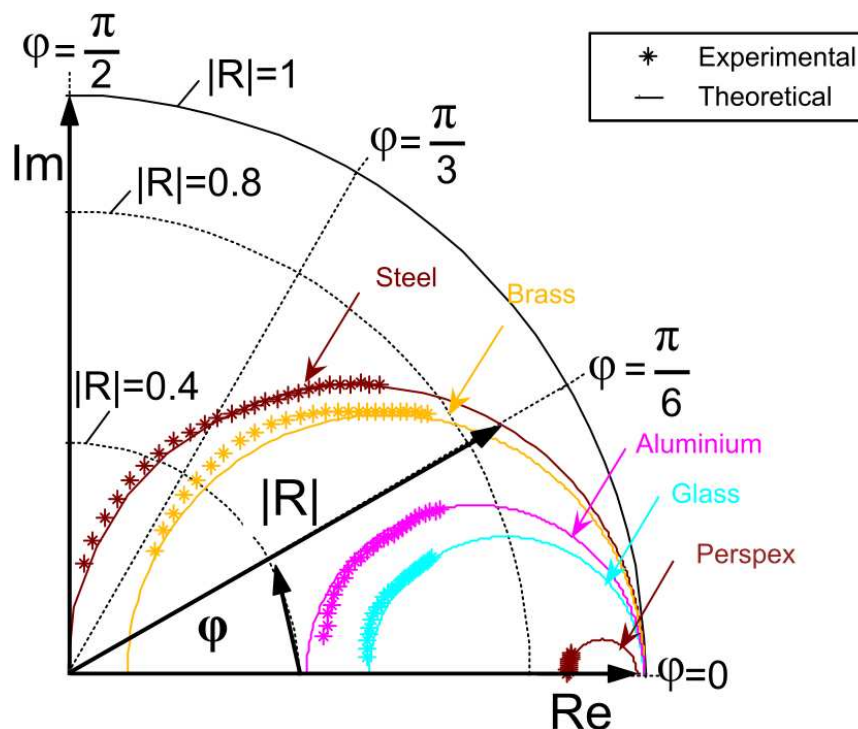


Figure 8. Argand diagram plotting complex reflection coefficient, showing how reflection coefficient varies with frequency from the experimental data.

Experimental results are over-plotted and give good agreement with the reflection coefficient locus. This means that, once again, the ultrasonic response of the thin layer system may be sufficiently represented by the spring model incorporating stiffness alone.

---

Figure 8 shows that the range of amplitude and phase both increase as the impedance of the specimen approaches that of the delay line (steel in this case). This suggests better accuracy is achieved under this condition. From the resulting impedances, there was no obvious correlation between accuracy and acoustic impedance of the measured specimen. Further study is required to determine how best to improve accuracy.

## **7. Discussion**

### *7.1. Experimental Accuracy*

The technique presented demonstrates high accuracy measurements for multi-layer interfaces with flat surfaces. Results were within 2-5% of those found via the conventional acoustic velocity-density method. The difference may be attributed to potential uncertainties in either technique, such as the specimens not having perfectly uniform geometries for volume measurement. Also, an accurate acoustic impedance value for some materials such as glass is difficult to obtain in data sheets as the wide array of specifications vary greatly. The usefulness of the method is demonstrated as there is no suitable alternatives available to measure acoustic impedance in such systems.

Measurement accuracy was maximised in this investigation by taking an average over the full useful transducer frequency spectrum. If required, accuracy could be improved further by also averaging measurements using multiple oil layer thicknesses.

Furthermore, the present study has demonstrated that density measurements may also be derived by this method if the length of the specimen is known and subsequent reflections are clear and distinct. Compared against measurements obtained via the mass-volume method, results varied by around 4% to 7%. As with acoustic impedance values, it is expected these differences are primarily due to uncertainties in both methods.

### *7.2. Practical Implementation of the Technique in Tribology*

The key advantage of the method presented is that it does not require knowledge of the oil film thickness and is independent of acoustic wave frequency. Thus, the method is particularly robust, with very little technical skill required to position the transducer onto a component and perform measurements. Additionally, the method does not require any form of calibration as it is based on a theoretical relationship.

Many tribological systems such as seals, bearings and piston ring-liner interfaces follow the configuration presented in this study, with two solids separated by a thin layer of liquid lubricant. Ultrasonic methods to measure film thickness in such components are becoming increasingly popular, however many of the established techniques require the acoustic impedance of both materials to be known. This method could be easily applied to determine acoustic impedance of the components without any additional hardware except what is already required for standard ultrasonic film thickness measurements.

The presented method may be equally useful in applications outside of tribology. For example, sintering processes require part density to deviate by no more than 1%, otherwise the component is deemed defective. Implementing a rapid quality assurance measurement technique could improve manufacturing efficiency and reduce waste.

## 8. Application to a Journal Bearing

The spring model has previously been used to measure the lubricating oil film thickness in journal bearing contacts [22, 24, 26]. However, for this, accurate acoustic impedance values for both media either side of a lubricated contact are required [26].

An automotive engine journal bearing shell is typically a layered construction with a thin steel shell and a single or multi-layer coating of soft metal alloys (sometimes known as white metal). The acoustic properties of the white metal layer are difficult to determine.

In the following, the acoustic impedance of a thin shell bearing coated with a white metal babbitt layer ( $\text{PbSn}_{10}\text{Cu}_3$ ) is calculated. This is achieved by measuring the change in phase and amplitude as the shaft rotates around the bearing circumference using the approach derived in section 2.

### 8.1. Test apparatus

Figure 9 shows the journal bearing test apparatus. An electric motor drives the steel shaft with a maximum rotation speed of 1500 rpm. Load is applied via a hydraulic jack on a stirrup system, up to 20 kN. Ultrasonic measurements were obtained via a 7 MHz longitudinal transducer embedded within the shaft, photographed in figure 10. A photograph of a bearing shell half used in this investigation is shown in figure 11, along with a schematic of the journal bearing system. A summary of key system dimensions and parameters are presented in table 3.



Figure 9. Photograph of journal bearing test rig.

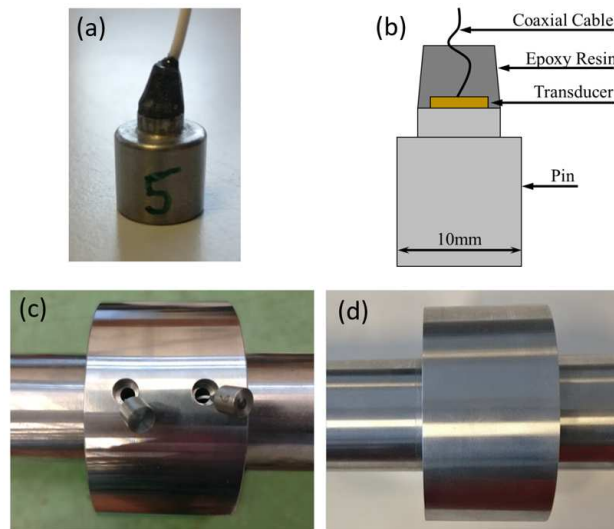


Figure 10. (a) Photograph of instrumented pin. (b) Schematic of instrumented pin. (c) Photograph of shaft pin installation. (d) Photograph of shaft after grinding.

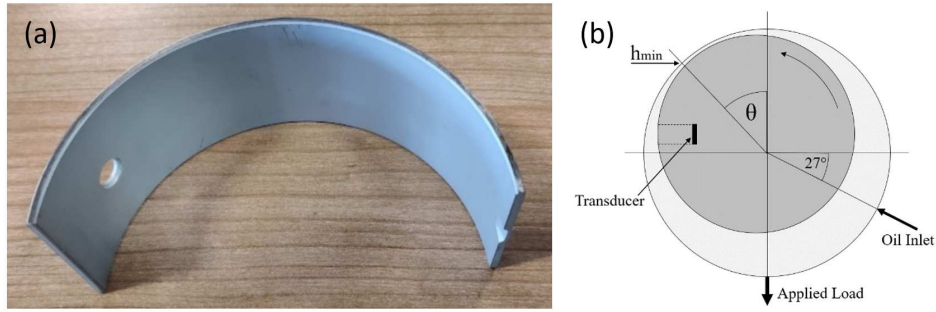


Figure 11. (a) Photograph of 112mm inner diameter journal bearing shell prior to installation. (b) Schematic of journal bearing system with the location of the shaft embedded ultrasonic transducer and oil inlet indicated.

Table 3. A summary of key bearing system dimensions and parameters

Parameter	Value
Bearing diameter	112 mm
Bearing width	50.55 mm
Bearing radial clearance	50 $\mu\text{m}$
White metal babbitt thickness	0.4 mm (approx.)
Lubricant kinematic viscosity	104 cSt @ 40°C, 11.6 cSt @100°C
Lubricant viscosity index	102
Lubricant density	888 kg/m <sup>3</sup>
Applied load	2 kN to 20 kN
Shaft rotation speed	100 rpm to 1500 rpm
Ultrasonic acquisition rate	80 kHz
Transducer centre frequency	7 MHz

### 8.2. Determination of Acoustic Impedance

Previous investigations have demonstrated that a reference measurement can be taken during operation provided the film is sufficiently thick [24, 27]. In this ‘thick film region’ reflection coefficient tends to a fixed value, depending only on the impedance mismatch between the shaft and the lubricant. The reference reflection coefficient amplitude can be calculated via equation 2, in which  $z_1$  and  $z_2$  are the impedance values of the shaft and lubricant respectively. Similarly, phase tends to zero as film thickness increases [28]. Thus, a reference can be obtained for every full rotation, taken at the point of maximum film thickness.

The exact thickness at which the oil film can be deemed sufficiently thick depends upon transducer centre frequency, lubricant density, and lubricant acoustic velocity. For this system, a film thickness exceeding 50  $\mu\text{m}$  can be defined as sufficiently thick. When compared against an infinitely thick film, this corresponds to a phase difference smaller than 0.025 radians and a reflection coefficient amplitude change under 0.001, both of which are lower than the practical measurement resolution of the system. As bearing radial clearance is 50  $\mu\text{m}$ , the maximum film around the bearing radial circumference will always be at least 50  $\mu\text{m}$ , thus a thick film reference can always be obtained regardless of operating conditions. A previous investigation

using the bearing test platform presented in this work assessed the effectiveness of the thick film measurement technique, concluding that this referencing method was more accurate than traditional pre-test referencing methods [24]. The primary benefit being that the reference and measurement are taken near-simultaneously. This overcomes the problem in that the energy output of piezoelectric elements can change over time, particularly when subjected to repeated elevated temperatures. Signal noise can introduce uncertainty into the reference measurement, which would thereby affect acoustic impedance measurements. To mitigate this, an average of thick film reference measurements taken over multiple rotations is taken for each test.

An advantage of this acoustic impedance measurement technique is that knowledge of the lubricant acoustic impedance, density or acoustic velocity are not required to determine bearing acoustic impedance. This is demonstrated in equation (12), in which these terms are not present. As such, any pressure or temperature effects on the lubricant do not need to be considered at this stage.

In this investigation, a total of 80 tests under a range of loads, rotations speeds and temperatures were performed.

Figure 12, which shows acoustic impedance around a section of the bearing circumference for an example test case, demonstrates that  $z_2$  remains consistent within the full converging region. As expected, the signal-noise ratio improves towards minimum film thickness. This is due to the non-linear relationship between film thickness and amplitude or phase; such that for very thin films a large change in amplitude or phase corresponds to a small change in thickness, whereas for thicker films a small change in either value corresponds to a large change in thickness.

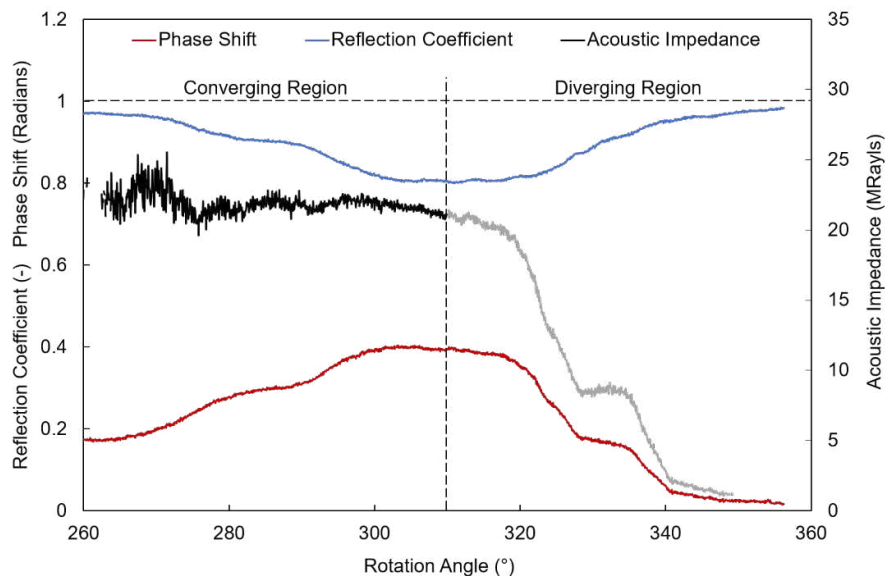


Figure 12. Acoustic impedance calculated by observing phase change and reflection coefficient within the minimum film region for an example test case (20 kN, 100 rpm at 65°C). Vertical dashed line represents the location of minimum film thickness.

Theoretically, any data point within the converging region can be used to obtain a value for bearing acoustic impedance, and for any test condition, such as any speed, load or bearing temperature. Although, measurements in the diverging region should be avoided due to cavitation effects introducing air bubbles into the lubricant. The accuracy of the technique is expected to improve with thinner films, as signal to noise ratio increases. Therefore, the optimum value would be at the point of minimum film thickness.

Figure 13 shows calculated acoustic impedance at the point of minimum film thickness compared against different variables: Sommerfeld number, temperature, load, and speed. The Sommerfeld number is a non-dimensional parameter used to equate oil film behaviour across bearings of different geometries [29] and can be expressed by the following formula:

$$S = \left(\frac{r}{c}\right)^2 \frac{\mu L D N}{F} \quad (15)$$

Where  $r$  is bearing radius,  $c$  is radial clearance between the shaft and bearing,  $\mu$  is dynamic viscosity,  $L$  is bearing length,  $D$  is bearing diameter,  $N$  is shaft rotation speed and  $F$  is applied load.

The calculated mean acoustic impedance was 24.36 MRayl, with a standard error of 0.23 MRayl ( $\pm 1\%$  of the mean). Results were analysed for normality and found to be normally distributed. A parametric Pearson correlation analysis was performed to determine whether any significance between any test conditions and acoustic impedance were present. None was found for Sommerfeld number, rotation speed or load ( $P=0.5692$ ,  $P=0.2608$ ,  $P=0.4723$  respectively). This is also demonstrated by the low R-squared values obtained via a linear regression, also presented in figure 13.

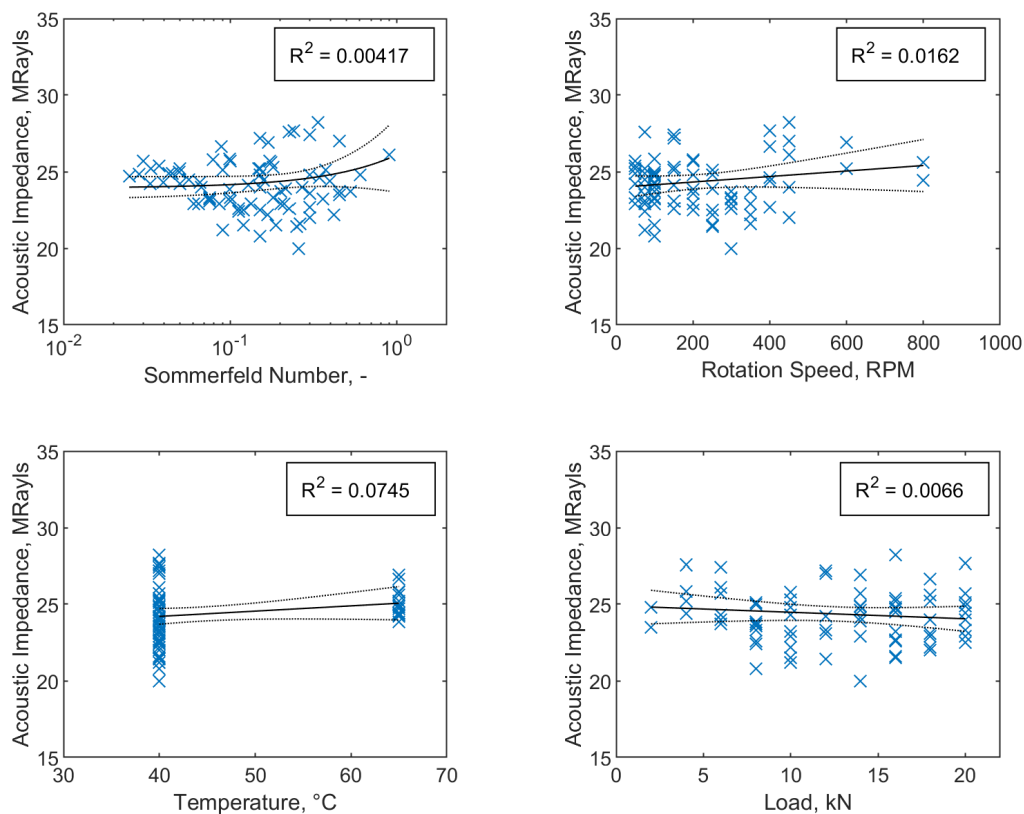


Figure 13. Acoustic impedance against Sommerfeld number (top-left), rotation speed (top-right), temperature (bottom-left) and load (bottom-right). Linear regression curve fits, along with corresponding  $R^2$  values are also presented.

A statistically significant link between  $z_2$  and temperature is shown ( $P=0.0143$ ), indicating that the observed positive correlation is not due to random sampling. With regards to the strength and magnitude of this association, the gradient and shared variance, quantified by R-squared (in this case 0.0745), are both low. The correlation observed could be explained by either a minor change in acoustic velocity, density, or both. Therefore, it is suggested this is not a measurement error but a true variation in acoustic impedance with temperature. For simplicity, as the change in  $z_2$  is low over the operating temperature range in this study, a constant value

for acoustic impedance can be used. Although this may need to be considered if testing systems over a wider range of temperatures.

Figure 13 also shows a reasonably wide distribution in individual acoustic impedance measurements compared to the more consistent static tests. This indicates that a single test would be insufficient for acoustic impedance measurement, particularly at lower temperatures. The standard deviation for tests at 40°C was 1.75 MRayls, whereas at 65°C the standard deviation was 0.92 MRayls. It is expected that standard deviation at higher temperatures is improved as this corresponds to thinner lubricant films when all other conditions are the same, such as shaft rotation speed and applied load.

The thickness of the bearing white metal layer is far too small for traditional acoustic impedance calculation techniques, particularly as the two reflections are not adequately separated for a clear time-of-flight measurement to be taken. However, this new technique has succeeded in obtaining a value. 24.36 MRayl is reasonable and within the region one may expect for white metals containing tin. Using literature values for density [30] and acoustic velocity [31], then applying equation 1, a typical tin-based white metal layer has a calculated acoustic impedance value of 24.8 MRayls, which is within 2% of the measured acoustic impedance of the white-metal layer used in this study.

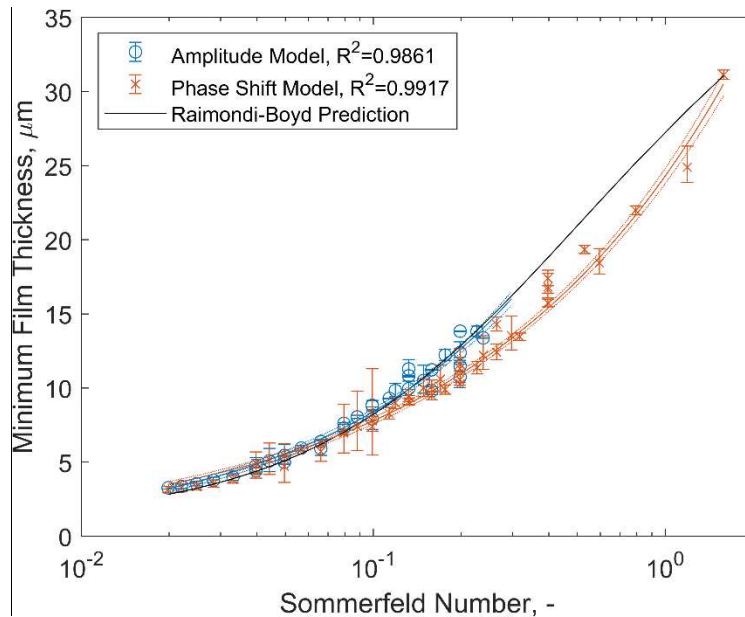
### 8.3. Calculating Lubricant Film Thickness using Acoustic Impedance

The calculated acoustic impedance value enables the measurement of film thickness,  $h$ , using the ultrasonic spring amplitude and phase models, as shown in equation 16 and equation 17 respectively [24]:

$$h = \frac{\rho c^2}{\omega z_1 z_2} \sqrt{\frac{R^2(z_2 + z_1)^2 - (z_2 - z_1)^2}{1 - R^2}} \quad (16)$$

$$h = \frac{\rho c^2 \tan(\Phi_R)(z_1^2 - z_2^2)}{\omega z_1 z_2^2 \pm \sqrt{(\omega z_1 z_2^2)^2 - \tan^2(\Phi_R)(z_1^2 - z_2^2)(\omega z_1 z_2)^2}} \quad (17)$$

This has been performed in figure 14, which shows minimum film thicknesses calculated via the amplitude and phase methods, along with a Raimondi Boyd numerical prediction [31]. Both the spring amplitude and phase model results agree with the numerical prediction, particularly for thinner films.



---

Figure 14. Minimum film thickness against Sommerfeld number for bearing testing under normal operating conditions. Theoretical prediction curve is obtained via the Raimondi-Boyd solution [31], measurements are obtained via the ultrasonic spring amplitude and phase shift methods. Error bars indicate variations in film measurement within each test case to  $\pm 1$  SEM.

Log-log nonlinear regression fits for each method are presented, along with dashed lines representing 95% confidence bands.

The calculated bearing acoustic impedance value enabled film thickness measurements via the amplitude spring model and phase models with low uncertainty, indicated by the narrow confidence bands in figure 14.

#### *8.4. Further Applications in Bearing Systems*

An additional potential use for this technique could be in condition monitoring. One could measure the acoustic impedance regularly to observe any significant change in value. An increase in acoustic impedance in this example may indicate that the white metal layer has worn, with the contact transitioning to a steel-steel interface. A further study would be required to investigate this, and it would be interesting to observe whether any change occurs before other signs of damage arise, such as increase in temperature or torque.

---

## Conclusions

The relationship between amplitude and phase of an ultrasonic wave reflected at a thin layer depends on the acoustic properties of the materials either side and is independent of layer itself. This has been used in a new approach for measuring the acoustic impedance of a solid medium which presents only one face.

The method is demonstrated experimentally, measuring the acoustic impedances of a range of materials. Results compare well with values determined conventionally from speed of sound and density (errors of 2-5%). If the sound path in the specimen is known, then it is possible to use the technique to measure density. Density values found in this way vary by 2-7% from those found from weight and geometry.

Dynamic measurements within a journal bearing contact have also been performed under a range of test conditions. Results indicated that acoustic impedance calculated using this method was not affected by the thickness of the oil layer. This has been applied to obtain high accuracy film thickness measurements via the amplitude and phase models.

The strength of the technique is that it can measure any value of acoustic impedance regardless of the specimen's attenuation, and geometry providing the specimen presents a flat face. Also, the technique does not require the thickness of the coupling layer to be known. Although this investigation applied the technique using longitudinal transducers, the authors see no reason why the approach would not be equally applicable to shear waves. The relation between acoustic impedance and reflection coefficient shown in equation (3) holds for both wave types, thus the procedure would be identical. This could widen the utility of this method to applications such as investigating the properties of matching layers used in viscosity measurements [33].

## Acknowledgements

The authors are grateful to Mr Auliver Brogan (Fermat) for his help in some of the modelling aspects of this work. The authors are also grateful to the Engineering and Physical Sciences Research Council for Prof. Rob Dwyer-Joyce's fellowship on Tribo-Acoustic Sensors EP/N016483/1; and the EPSRC Centre for Doctoral Training in Integrated Tribology EP/L01629X/1. The authors would also like to thank Mr David Butcher for his help in the design and commissioning aspects of the journal bearing test platform presented in this work.

## References

- [1] Krautkramer, J., and Krautkramer, H. (1977). *Ultrasonic Testing of Materials*. New York, Springer-Verlag.
- [2] S. Hoche, M. A. Hussein, and T. Becker, (2015). "Density, ultrasound velocity, acoustic impedance, reflection and absorption coefficient determination of liquids via multiple reflection method," *Ultrasonics*, vol. 57, no. C, pp. 65–71, doi: 10.1016/j.ultras.2014.10.017.
- [3] F. Bianco, L. Fredianelli, F. Lo Castro, P. Gagliardi, F. Fidecaro, and G. Licitra, (2020). "Stabilization of a p-u sensor mounted on a vehicle for measuring the acoustic impedance of road surfaces," *Sensors (Switzerland)*, vol. 20, no. 5, pp. 1–16, doi: 10.3390/s20051239.
- [4] M. Yu, L. Shen, T. Mutasa, P. Dou, T. Wu, and T. Reddyhoff, (2020). "Exact analytical solution to ultrasonic interfacial reflection enabling optimal oil film thickness measurement," *Tribol. Int.*, vol. 151, doi: 10.1016/j.triboint.2020.106522.

- 
- [5] S. Alam and R. I. Marshall, (1992). "The testing performance of various bronze bushes," *J. Phys. D. Appl. Phys.*, vol. 25, no. 9, pp. 1340–1344, doi: 10.1088/0022-3727/25/9/010.
- [6] R. Ferreira, R. Almeida, Ó. Carvalho, L. Sobral, S. Carvalho, and F. Silva, (2021). "Influence of a DLC coating topography in the piston ring/cylinder liner tribological performance," *J. Manuf. Process.*, vol. 66, no. April, pp. 483–493, doi: 10.1016/j.jmapro.2021.04.044.
- [7] Rooke, J., Li, X., Brunskill, H., Stark, M. et al., (2021). "Comparison of Ring-Liner Oil Film Thickness Resulting from Different Injector Designs in a Diesel Marine Engine Using an Ultrasound Measurement Method," *SAE Int. J. Engines* 14(6), <https://doi.org/10.4271/03-14-06-0053>.
- [8] P. Harper, B. Hollingsworth, R. Dwyer-Joyce, and B. Drinkwater, (2003). "Journal bearing oil film measurement using ultrasonic reflection," in *Proceedings of the 29th Leeds-Lyon Symposium on Tribology*, vol. 41, pp. 469–476, doi: 10.1016/S0167-8922(03)80161-X.
- [9] Filipczynski, L., Z. Pawlowski, and Wehr, J. (1966). *Ultraonic Testing of Materials*. London, Butterworths.
- [10] Mason, W. P., and Thurston, R. N. (1979). *Physical Acoustics*. New York, Academic Press, pp. 505-509.
- [11] Perdrix, M., Baboux J.-C., and Lakestani, F. (1981). "Acoustic Impedance Measurement by Reflection of an Ultrasonic Impulse on a Specimen through a Coupling Layer." *IEEE Trans Sonics Ultrason*, Vol 28(6), pp. 431-436
- [12] Tattersall, H.G., (1973). the ultrasonic pulse-echo technique as applied to adhesion testing, *J.Appl. Phys.D.*, Vol. 6, pp. 819-832.
- [13] Schoenberg, M. (1980). Elastic wave behavior across linear slip interfaces. *Journal of the Acoustical Society of America*, 68(5), 1516–1521. <https://doi.org/10.1121/1.385077>
- [14] Pialucha, T., and P. Cawley (1994). The detection of embedded layers using normal incidence ultrasound, *ASLE Trans.*, 32(6): 337-348
- [15] Nagy, P. B. (1992). Ultrasonic classification of imperfect interfaces, *J. Nondestr. Eval.*, Vol. 11, pp. 27-137.
- [16] Haines, N. F., (1980). The theory of sound transmission and reflection at contacting surfaces, Report RD/B/N4744, CEGB Research Division, Berkeley Nuclear Laboratories.
- [17] Baltazar, A., Rokhlin, S. I., and Pecorari, C., (2002). On the relationship between ultrasonic and micromechanical properties of contacting rough surfaces. *J.Mech. Phys.* Vol. 50, pp. 1397-1416.
- [18] Kendall, K. and Tabor, D., (1971). An ultrasonic study of the area of contact between stationary and sliding surfaces, *Proc. R. Soc. Lond. A*, Vol. 323, pp. 321-340.
- [19] Krolkowski, J. and Szczepek J., (1991). Prediction of contact parameters using ultrasonic method, *Wear*, Vol. 148, pp. 181-195.
- [20] Carretta, Y., Hunter, A. K., Boman, R., Ponthot, J. P., Legrand, N., Laugier, M., & Dwyer-Joyce, R. S. (2017). Ultrasonic roll bite measurements in cold rolling – Roll stress and deformation. *Journal of Materials Processing Technology*, 249 (December 2016), 1–13. <https://doi.org/10.1016/j.jmatprotec.2017.05.036>
- [21] Brunskill, H., Hunter, A., Zhou, L., Dwyer Joyce, R., & Lewis, R. (2020). An evaluation of ultrasonic arrays for the static and dynamic measurement of wheel–rail

- 
- contact pressure and area. *Proceedings of the Institution of Mechanical Engineers, Part J: Journal of Engineering Tribology*, 234(10), 1580–1593.  
<https://doi.org/10.1177/1350650120919889>
- [22] Ouyang, W., Zhou, Z., Jin, Y., Yan, X., & Liu, Y. (2020). Ultrasonic measurement of lubricant film thickness distribution of journal bearing Ultrasonic measurement of lubricant film thickness distribution of journal bearing. *Review of Scientific Instruments*, 065111(March). <https://doi.org/10.1063/5.0007481>
- [23] Zhang, K., Dou, P., Wu, T., & Feng, K. (2019). An ultrasonic measurement method for full range of oil film thickness. *Engineering Tribology*, 233(3), 481–489.  
<https://doi.org/10.1177/1350650118787038>
- [24] Beamish, S., Li, X., Brunskill, H., Hunter, A., & Dwyer-Joyce, R. (2020). Circumferential film thickness measurement in journal bearings via the ultrasonic technique. *Tribology International*, 148(February), 106295.  
<https://doi.org/10.1016/j.triboint.2020.106295>
- [25] Kasolang, S. & Dwyer-Joyce, R.S. (2008). Viscosity measurement in thin lubricant films using shear ultrasonic reflection. *Proceedings of the Institution of Mechanical Engineers, Part J: Journal of Engineering Tribology*, 222(3),423-429.
- [26] S. Kasolang and R. S. Dwyer-Joyce, (2008). “Observations of Film Thickness Profile and Cavitation Around a Journal Bearing Circumference,” *Tribol. Trans.*, vol. 51, no. 2, pp. 231–245, doi: 10.1080/10402000801947717.
- [27] Dwyer-Joyce, R.S., Drinkwater, B.W., and Donohoe, C.J., (2002). The Measurement of Lubricant Film Thickness using Ultrasound, *Proc Royal Soc A*, Vol. 459, pp 957-976.
- [28] Reddyhoff, T., Kasolang, S., Dwyer-Joyce, R. S., & Drinkwater, B. W. (2005). The phase shift of an ultrasonic pulse at an oil layer and determination of film thickness. *Proceedings of the Institution of Mechanical Engineers, Part J: Journal of Engineering Tribology*, 219(6), 387–400. <https://doi.org/10.1243/135065005X34044>
- [29] Stachowiak, G., & Batchelor, A. (2006). *Engineering Tribology. Engineering Tribology* (Third). Elsevier. <https://doi.org/10.1016/B978-0-08-097053-0.00001-7>
- [30] *Metals and Alloys in the Unified Numbering System*, (1999), 8th ed., Society of Automotive Engineers, Inc. and American Society for Testing and Materials.
- [31] Olympus, “Ultrasonic Inspection of Babbitt Bearing Liners.” <https://www.olympus-ims.com/en/ultrasonic-inspection-babbitt-bearing-liners/> (accessed Jan. 11, 2022).
- [32] J. Raimondi, A. A. and Boyd. (1958). “A Solution for the Finite Journal Bearing and its Application to Analysis and Design,” *ASLE Trans.*, vol. 1, no. 1, pp. 159–174, doi: 10.1080/05698195808972328.
- [33] Schirru, MM, Dwyer-Joyce, & RS. (2015). A model for the reflection of shear ultrasonic waves at a thin liquid film and its application to viscometry in a journal bearing. *Part J: Journal of Engineering Tribology*, 230(6), 667–679.  
<https://doi.org/10.1177/1350650115610357>